Electronic Supporting Information (ESI)

Design and Electrospinning Synthesis of Red Luminescent-Highly Anisotropic Conductive Janus Nanobelt Hydrogel Array Film

Haina Qi[1, *], Huazhi Huang[1], Yaolin Hu[2], Ning Li[1], Liu Yang[3], Xuejian Zhang[1, *], Yongtao Li[1], Hongkai Zhao[1], Dan Li[2], Xiangting Dong[2, *]

1. School of Materials Science and Engineering, Ji Lin Jian Zhu University, Changchun 130018, China

2. Key Laboratory of Applied Chemistry and Nanotechnology at Universities of Jilin Province, Changchun University of Science and Technology, Changchun 130022, China

3. School of Materials Science and Engineering, Heilongjiang University of Science and Technology, Harbin 150001, China

Fax: 86 0431 85383815; Tel: 86 0431 85582574; E-mail: zxj_0620@163.com (Xuejian Zhang); xtdong@cust.edu.cn (Xiangting Dong); qihaina@jlju.edu.cn (Haina Qi);

Experiments

Chemicals

Gelatin (GE), carbon black (CB), hexafluoroisopropanol (HFIP), Eu_2O_3 (99.99 %), triphenylphosphine oxide (TPPO, 98 %), 2-thiophenoyltrifluoroacetone (HTTA, 98 %), HNO_3, $NH_3 \cdot H_2O$, glutaraldehyde (GA, 50 %), anhydrous ethanol, phosphate buffer solution (PBS), NaOH and HCL were used, and all of the chemicals were of analytic grade and purchased from Aladdin reagent Co. LTD, Shanghai, China. Ultrapure water was prepared by Mili-QAdvantageA10 ultrapure water machine in our laboratory.

Preparation and forming principle of [Eu(TTA)$_3$(TPPO)$_2$/GE]//[CB/GE] Janus nanobelt array film and hydrogel film

Two different spinning solutions were prepared to construct [Eu(TTA)$_3$(TPPO)$_2$/GE]//[CB/GE] Janus nanobelt array film (denoted as JAF). The compositions and concentrations of spinning solution I and spinning solution II are shown in Table S1 and S2.

Table S1 Compositions of the spinning solution I.

Spinning solution Ⅰ	Eu(TTA)$_3$(TPPO)$_2$/GE /wt %	Eu(TTA)$_3$(TPPO)$_2$ (g)	GE (g)	HFIP (mL)
Ⅰ$_{E-1}$	10	0.10	1.00	10
Ⅰ$_{E-2}$	15	0.15	1.00	10
Ⅰ$_{E-3}$	20	0.20	1.00	10
Ⅰ$_{E-4}$	25	0.25	1.00	10

Table S2 Compositions of the spinning solution II.

Spinning solution Ⅱ	CB/GE/wt %	CB (g)	GE (g)	HFIP (mL)
Ⅱ$_{C-1}$	1	0.01	1.00	10
Ⅱ$_{C-2}$	3	0.03	1.00	10
Ⅱ$_{C-3}$	5	0.05	1.00	10
Ⅱ$_{C-4}$	7	0.07	1.00	10

Characterization techniques

The morphology and microstructure of the samples were observed using an optical microscope (OM, CVM500E) and a scanning electron microscope (SEM, JSM-7610F). Elemental analysis of the films was performed by energy dispersive spectroscopy (EDS, Oxford Instruments). The luminescence properties of the samples were analyzed using a luminescence spectrometer (Hitachi F7000) with the slit widths of excitation and emission set at 2.5 nm, respectively. The electrical conductivity of the samples was measured by an LCR digital bridge (TH2810B+). The FTIR spectra were recorded by an infrared spectrophotometer (Nicolet iS5) using the KBr disk technique. The thermal stability of the samples was measured by thermogravimetric analyzer (TGA500, TA Instruments, USA). The mechanical properties of the samples were measured by a microcomputer-controlled electronic universal testing machine (WDW-20 kN). The PHI 5000 VersaProbe X-ray photoelectron spectrometer (XPS) was used to analyze quantitatively the composition of the elements and the valence state of the elements in the samples. The XPS was produced by ULVCA-PHI Company and mono X-ray source was Al Kα excitation, the full spectrum scan ranged from 0 eV to 1200 eV. All the above measurements were performed at room temperature.

Mechanical performance

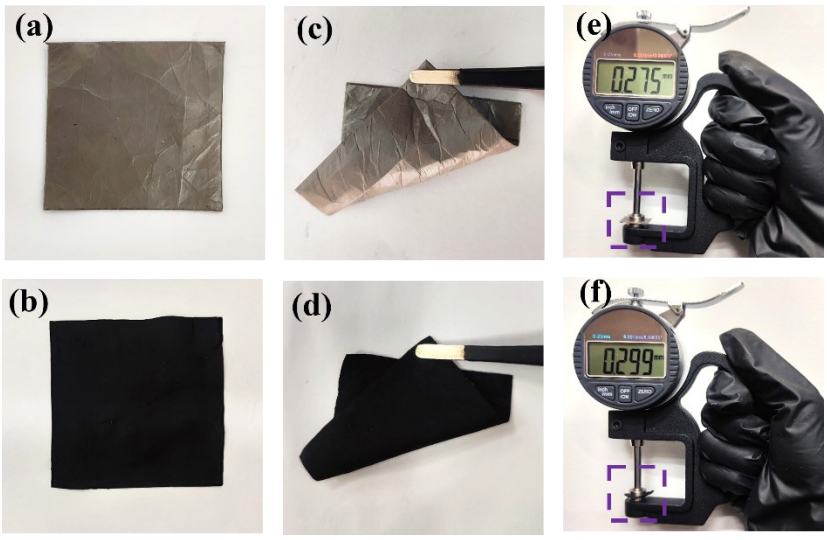

Figure S1 Plane, bending and thickness test physical drawings of JAF (a, c, e) and JAHF (b, d, f).

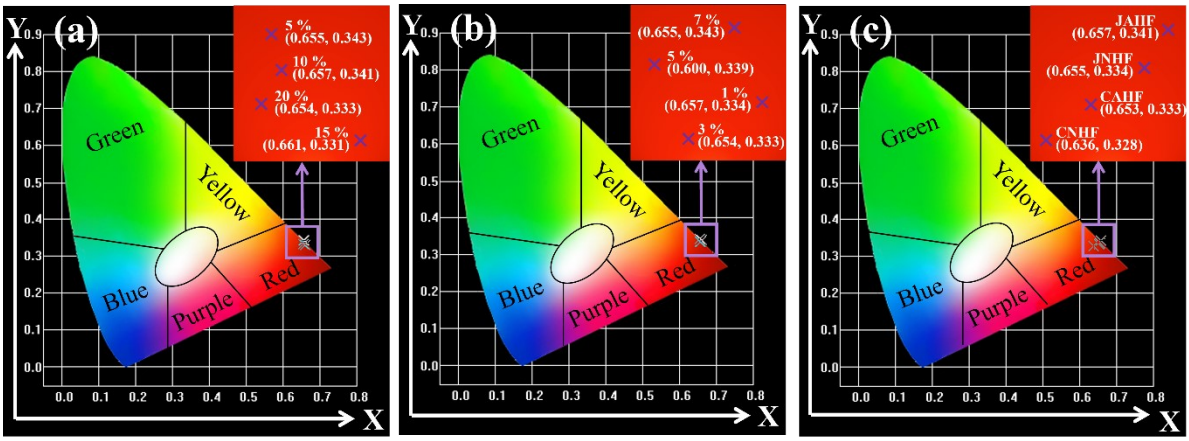

Figure S2 CIE chromaticity coordinates of JAHF with different $Eu(TTA)_3(TPPO)_2$ contents (a) and CB contents (b), and the comparison samples (c) under 344 nm optical excitation.

Table S3 Specific resistance and conductance values of samples.

Samples	CB/GE /wt %	SX	SY	SX/SY	Anisotropy degree
JAHF	1	3.01×10^{-7}	1.12×10^{-9}	2.69×10^{2}	Weak
JAHF	3	3.35×10^{-6}	2.72×10^{-9}	1.23×10^{3}	Medium
JAHF	5	1.70×10^{-5}	1.01×10^{-9}	1.69×10^{4}	Strong
JAHF	7	2.43×10^{-4}	1.60×10^{-9}	1.52×10^{5}	Very strong
JNHF	3	1.06×10^{-6}	1.32×10^{-6}	0.80	None
CAHF	3	7.95×10^{-6}	3.98×10^{-6}	2.00	Very Weak
CNHF	3	1.50×10^{-6}	2.11×10^{-6}	0.71	None

Table S4 Comparison of the properties of the present work with other anisotropic conducting hydrogels.

Hydrogel network	Conductance		Anisotropic	Time	Reference
	Parallel	Perpendicular			
GE/CB	2.43×10^{-4} S	1.60×10^{-9} S	1.52×10^{5}	2024	This work
PVA/PEDOT: PSS	--	--	60.8	2024	39
PVA-PAA/Fe^{3+}	634.64 mS m^{-1}	169.09 mS m^{-1}	3.75	2024	40

PNIPAM/CFs	670 S m^{-1}	1.6 S m^{-1}	400	2023	41
PAA/PAM/GI	1.5 S m^{-1}	0.24 S m^{-1}	6	2023	42
PVA/CNTs/TA	20.4 S m^{-1}	9.3 S m^{-1}	2.19	2023	43
SA/PAM-PAA/Fe^{3+}	401 mS m^{-1}	239 mS m^{-1}	1.68	2023	44
PAAm/SA/MXene/$ZrOCl_2$	0.096 S m^{-1}	0.058 S m^{-1}	1.67	2023	45
PVA/CS/AMPS	1.21 S m^{-1}	0.78 S m^{-1}	1.55	2023	46
PPY	30 S cm^{-1}	6 S cm^{-1}	5	2021	47
PVA/MXene/$ZnSO_4$	56 mS m^{-1}	--	1.3	2021	48
BC/PEDOT/PSS	6.62×10^{-3} S cm^{-1}	1.61×10-3 S cm^{-1}	4.1	2020	49
PDA/Fe_3O_4 NPs/CNT	0.51 S m^{-1}	0.32 S m^{-1}	1.90	2019	50